Neighbor-directed histidine N (#)-alkylation: A route to imidazolium-containing phosphopeptide macrocycles

Citation: Qian, Wen-Jian et al. "Neighbor-Directed Histidine N (τ)-Alkylation: A Route to Imidazolium-Containing Phosphopeptide Macrocycles: Neighbor-Directed Histidine N(τ)-Alkylation." Biopolymers 104.6 (2015): 663–673.

As Published: http://dx.doi.org/10.1002/bip.22698

Publisher: Wiley Blackwell

Persistent URL: http://hdl.handle.net/1721.1/105840

Version: Author's final manuscript: final author's manuscript post peer review, without publisher's formatting or copy editing

Published in final edited form as:

Biopolymers. 2015 November ; 104(6): 663–673. doi:10.1002/bip.22698.

Neighbor-directed Histidine N(τ)–Alkylation: A Route to Imidazolium-containing Phosphopeptide Macrocycles

Wen-Jian Qian[1], **Jung-Eun Park**[2], **Robert Grant**[3], **Christopher C. Lai**[1], **James A. Kelley**[1], **Michael B. Yaffe**[3], **Kyung S. Lee**[2], and **Terrence R. Burke Jr.**[1,*]

[1]Chemical Biology Laboratory, Center for Cancer Research, National Cancer Institute-Frederick, Frederick, MD 21702

[2]Laboratory of Metabolism, Center for Cancer Research, National Cancer Institute, National Institutes of Health, Bethesda, MD 20892

[3]Department of Biology and Biological Engineering, Center for Cancer Research, Massachusetts Institute of Technology, Cambridge, MA 02139

Abstract

Our recently discovered, selective, on-resin route to N(τ)-alkylated imidazolium-containing histidine residues affords new strategies for peptide mimetic design. In our current work, we demonstrate the use of this chemistry to prepare a series of macrocyclic phosphopeptides, in which imidazolium groups serve as ring-forming junctions. Interestingly, these cationic moieties subsequently serve to charge-mask the phosphoamino acid group that directed their formation. Neighbor-directed histidine N(τ)-alkylation opens the door to new families of phosphopeptidomimetics for use in a range of chemical biology contexts.

Keywords

Plk1; polo kinase; polo-box domain; crystal structure; cationic dialkyl histidine; peptide macrocycles; phosphopeptides

INTRODUCTION

Modification of amino acid residues in biologically active peptides is a powerful tool for peptidomimetic design. These efforts can be greatly facilitated by transforming reactions that are selective and can be performed on solid-phase resin. Histidine is unique among the coded amino acids in having an imidazole ring with its two associated unsubstituted nitrogen atoms. Yet, exploiting histidine's full potential for constructing peptidomimetics has been limited by the challenges of differentially functionalizing its N(π)- and N(τ)-positions. We have recently discovered the unanticipated ability of phosphoamino acids to direct the N(τ)-

*Corresponding author: Terrence R. Burke, Jr., Ph.D., National Cancer Institute, National Institutes of Health, Building 376 Boyles St., NCI-Frederick, Frederick, MD 21702, U.S.A., Phone: (301) 846-5906; Fax: (301) 846-6033, tburke@helix.nih.gov.

SUPPORTING INFORMATION

Supporting Information includes mass spectral characterization of product macrocycles and selected precursors and X-ray crystallography refinement data and SigmaA weighted 2Fo–Fc electron density maps for Plk1-bound **3b**, **3c** and **4c**.

alkylation of proximal histidine residues already bearing an N(π)-substituent.[1,2] These reactions are highly selective and can be conducted on fully protected peptides bound to solid-phase resin using Mitsunobu chemistries. The facile access to N(π), N(τ)-derivatized histidine residues affords as yet unexplored access to new families of peptidomimetics.

In the first practical application of this technology, we turned our attention to the sequence, "Ac-Pro-Leu-His-Ser-pThr-amide" (**1**, Figure 1), which is based on the C-proximal residues of the polo-box interacting protein 1 (PBIP1).[3] The polo-like family of serine/threonine kinases (Plks) plays critical roles in cell cycle regulation, and antagonists of Plk1 are being developed as potential anticancer agents. The Plks are characterized as having polo-box domains (PBDs), which recognize phosphothreonine (pThr) and phosphoserine (pSer)-containing sequences. In designing Plk1 PBD-binding antagonists, we had originally started with peptide **1** and found that adding long-chain alkylphenyl groups to the N(π) position of the His residue significantly enhances PBD-binding affinity.[4] It was in subsequent studies with peptides of the form, "Ac-Pro-Leu-His*-Ser-pThr-amide" (**2**, Figure 1), where "His*" indicates the presence of an N(τ)–$(CH_2)_8$Ph group, that we first observed the preferential alkylation at the His N(τ)-position under Mitsunobu conditions.[1] The formation of N(π), N(τ) bis-alkyl-His species was providential, since these peptides showed little or no diminution of PBD-binding affinity in *in vitro* assays, yet cellular potencies increased. This latter fact points to greater membrane transit made possible by intramolecular "charge-masking" of one anionic pThr phosphoryl hydroxyl by the bis-alkyl-His imidazolium cation.[5]

We anticipated that N(τ)–alkylation could serve as a specific means of introducing structural diversification into the His imidazole side chain,[2] and that such species could be employed for the construction of new classes of macrocyles. The importance of macrocyclization for constraining flexible ligands is widely recognized,[6–9] and using the bifurcated His residue for ring closure could provide advantages in the design of macrocyclic PBD-binding peptides relative to more standard methodologies.[10]

RESULTS AND DISCUSSION

In order to examine the application of phospho-dependent His N(τ)–alkylation for macrocyclization, we designed three families of cyclized variants based on the parent sequence **1** (**3** – **5**, Figure 1). We incorporated the requisite His* residues under standard Fmoc conditions using our recently reported reagent.[11] Macrocyclization was accomplished using ring-closing metathesis (RCM),[12] which required preparing the appropriate open-chain bis-alkenyl precursors. Amino-terminal alkenyl chains were appended either as ethers of *R*-4-hydroxy-Pro[13] (for peptides **3**) or as *N*-alkenoyl amides of Leu (peptides **4**) and His* (peptides **5**) (Figure 1).

Synthetic Approaches to Macrocycles 3, 4 and 5

Macrocycles 3a – 3d—Type **3** macrocycles were prepared in 18, 20, 22 and 24-member ring sizes (**3a**–**3d**, respectively, Figure 1). Resin-bound peptides having terminal Pro residues containing either an *R-4-*(4-pentenyloxy) or *R-4-*(2-propenyloxy) group (peptides **6a** and **6b**, respectively) were subjected to pThr-directed Mitsunobu alkylations of their His*

N(τ)–nitrogens using a series of alkenyl alcohols.[1,2] This afforded the requisite resin-bound bis-alkyl-His-containing peptides (**7a**–**7d**, Figure 2). On-resin microwave-assisted RCM ring closure using a common Pro residue having a 3-(4-pentenyloxy) group and the appropriate length N(τ)–alkenyl group was possible for the 20, 22 and 24-member macrocycles (**8b**–**8d**, respectively, Figure 2). Microwave irradiation can decrease reaction times, enhance catalyst performance and improve overall yields of RCM reactions.[14–19] Typically, these reactions are conducted in a solvent combination of CH_2Cl_2: dimethylformamide (DMF) (10:1) using 2nd Generation Grubbs[20] or Hoveyda-Grubbs[21] catalyst. The DMF facilitates peptide solubility and absorbs microwave radiation, while CH_2Cl_2 swells the resin.

During initial attempts to prepare the shorter 18-member macrocycle (**3a**) using 2-propenyl groups on both the 3-oxy-Pro and His*- N(τ) positions, it was found that on resin microwave-assisted RCM macrocyclization resulted in the loss of the Pro 3-alkoxy group, as was also the case when a Pro 3-butenyloxy group was employed. We rationalized that these losses could reflect Ru-catalyzed isomerization to a more labile 2-butenyl species.[22] We circumvented these difficulties by using a 1-cinnamoyl group at the N(τ)–position (**7a**), which served as a 2-propenyl surrogate.[23] In this fashion we obtained the desired 18-membered macrocycle (**11**) by solution-phase RCM of the precursor peptide (**10**) at room temperature following cleavage from the resin (Figure 2).

Because cyclization under RCM conditions typically yields mixtures of E/Z products,[24,25] we eliminated geometric isomers by reducing the ring-closing double bonds. We examined diimine reduction, since this is compatible with both solution and solid-support protocols.[26,27] We found that on-resin reduction of the 20-member macrocycle (**8b**) using 2-nitrobenzenesulfonohydrazine (NBSH) and NEt_3[26,27] resulted in poor conversion to the desired saturated macrocycle (**9b**). However, for the larger macrocycle ring sizes (22 and 24 member; **8c** and **8d**, respectively), we achieved good conversion to the desired products (**9c** and **9d**, respectively) using NBSH (20 equiv) and NEt_3 (40 equiv) in CH_2Cl_2 with microwave irradiation (50 °C, 30 min) Subsequently, we found that cleavage of resin-bound **8b** to give **11b** and hydrogenation in solution using H_2 over 10% Pd•C in tetrahydrofuran (THF):DMF (10:1) at room temperature (overnight) gave very high-yield conversion to the saturated product (**3b**). Ring closure required for the synthesis of the shorter 18-member macrocycle (**3a**) could not be performed on-resin, due to lability of the Pro allyloxy group under the microwave conditions needed for the on-resin RCM reaction. However, RCM cyclization could be achieved in solution at room temperature on **10** following cleavage of **7a** from the resin. This yielded the unsaturated macrocycle (**11a**), which was hydrogenated (H_2 over 10% Pd•C) to provide the desired final macrocycle **3a** (Figure 2).

Macrocycles 4a – 4e—Type **4** macrocycles, based on the “Leu-His*-Ser-pThr” motif, were prepared similar to that described above for type **3** macrocycles. Precursor open-chain peptides for 18, 20, 22 and 24-member macrocyles (**4b**–**4e**, respectively) were assembled on-resin by initial *N*-terminal acylation with either hex-5-enoic acid (**12a**) or oct-7-enoic acid (**12b**). The peptides were subjected to pThr-directed Mitsunobu N(τ)–alkylation using the appropriate alkenyl alcohols, pent-4-ene-1-ol (for **13b** and **13c**); hept-6-ene-1-ol (for **13d**) and none-8-ene-1-ol (for **13e**, Figure 3). On-resin RCM ring closures to the

corresponding peptides **14b**–**14e** were carried out as indicated above, using Hoveyda-Grubbs 2nd generation catalyst in CH_2Cl_2:DMF (10:1) with microwave irradiation (120 °C, 30 min). Diimine-mediated on-resin reduction of the resulting ring-forming double bonds yielded **15b**–**15e** [(20 and 40 equiv of NBSH and Et_3N, respectively in CH_2Cl_2 with microwave irradiation (50 °C, 30 min)]. The final macrocyclic peptides (**4b**–**4e**) were obtained by resin cleavage and high performance liquid chromatography (HPLC) purification (Figure 3). We found in the attempted synthesis of the 16-member type **4** macrocycle using *N*-terminal acylation with but-3-enoic acid, that on-resin microwave-assisted RCM macrocylization resulted in ring-contraction (loss of $–CH_2–$). This may have occurred by isomerization of the but-3-enoyl amide to the conjugated but-2-enoyl species prior to ring closure. Subsequent on-resin diimine reduction of the smaller, 15-member macrocycle also failed. However, cleavage of the peptide from the resin and followed by solution-phase reduction (H_2 over 10% Pd•C) gave the 15-member macrocycle (**4a**).

Macrocycles 5a – 5f—Syntheses of the "His*-Ser-pThr"–based type **5** macrocycles were achieved entirely on solid-phase. Ring sizes were determined by on–resin pThr-directed N(τ)–alkylation of peptides (**16a–16c**) with appropriate-length alcohols to give the corresponding series of bis-alkenyl-containing peptides (**17a–17f**) (Figure 4). Microwave irradiation was employed both for RCM macrocyclization (120 °C, 30 min) to yield the corresponding unsaturated macrocycles (**18a–18f**), and for the subsequent diimine double bond reduction (50 °C, 30 min). Cleavage of the saturated macrocycles (**19a–19f**) gave the desired final products **5a–5f**, having ring sizes of 14-, 16-, 18-, 20-, 22- and 24-members, respectively (Figure 4).

Mass Spectral Characterization

We had previously verified the structures of on-resin Mitsunobu His* N(τ)-alkylation products by high-resolution liquid chromatography – tandem mass spectrometry (LC/MS/MS) analyses using electrospray ionization (ESI).[2] We performed similar analyses for peptides of the current series. For all macrocyclic final products, both the protonated peptide (MH^+) and the double-protonated peptide $(M+2H)^{2+}$ ions were observed and had masses consistent with the expected elemental composition (see Supporting Information). Interestingly, the $(M+2H)^{2+}$ ions of these macrocycles were of consistently lower relative abundance than those observed in the ESI mass spectra of their linear analogues reported earlier.[2] The increased spatial constraint of these molecules may make multiple charging less energetically favored than with the linear pThr-containing pentapeptide derivatives. LC/MS/MS analysis also confirmed the presence of a free phosphate moiety and the absence of any macrocyclic derivatives resulting from RCM through the isomeric phosphate ester.

Typically, the primary low energy MS/MS fragmentation observed for pSer- and pThr-containing peptides is loss of neutral phosphoric acid (H_3PO_4) or HPO_3, with a much reduced fragmentation of the amide bond peptide backbone to generate b and y sequence-indicating ions.[28] The abundance of these ions depends on the charge-state of the precursor ion, the structure of the peptide and the nature of the collision-induced dissociation (CID).[29,30] For the macrocyclic phosphopeptide **3c**, which contains a ring-constrained, cationic bis-alkyl-His and a free phosphate, a predominant and diagnostic CID-mediated

neutral loss should be that of H_3PO_4 (98 da), resulting in a product ion at *m/z* 891.5702. Other prominent neutral losses are expected to be those that are related, such as MH^+-HPO_3 and MH^+-(H_3PO_4 + NH_3), as well as MH^+-NH_3 from the C-terminal amide. These product ions are all observed in the MS/MS spectrum resulting from CID of the MH^+ of **3c** (Figure 5 and Supporting Information). The b_n and y_n sequence-indicating ions for the macrocyclic pThr-containing peptide derivatives are also expected to be somewhat different from those of the linear analogues. Thus in the case of **3c**, the b_n ions that are seen are those that incorporate the cyclic His*-imidazolium cation, namely b'_3 and b'_4 (Figure 5). (Note that the b'_n ions observed for this and other macrocycles are designated by a prime to indicate a localized charge and numbered on the basis of amino acid residues in the cyclic His*-imidazolium cation.) Furthermore, because the macrocycle is formed through His*, no y_3 ions are seen for **3c**, since cleavage at the Leu-His* amide bond no longer results in a distinct y_n product ion. Thus, taken all together, the MS/MS spectrum of **3c** (Figure 5) and those of the other macrocyclic derivatives (Supporting Information) support structures containing a free phosphate and a macrocyclic ring formed through a His*-imidazolium cation.

Determination of Plk1 PBD-binding Affinities

PBIP1 is a physiological substrate of Plk1, that once phosphorylated at Thr78, forms a Plk1–PBIP1 complex through the interaction between the PBD of Plk1 and the pThr78 of PBIP1.[31] Peptide **1** represents residues 74–78 of PBIP1. In order to determine their Plk1 PBD-binding affinities, the synthetic macrocyclic peptides were evaluated in an enzyme-linked immunosorbent assay (ELISA)-based assay that measured their ability to compete with an immobilized pThr78-derived peptide for binding to human influenza hemagglutinin-green fluorescent protein (HA-GFP)- fused Plk1 expressed in HEK 293A cells. Consistent with our previous findings, introducing the N(π)–$(CH2)_8$Ph group (peptide **2**, IC_{50} = 12 nM) significantly increased binding affinity relative to the parent peptide (**1**, IC_{50} = 23 μM) (Table 1).[4] In the type **3** macrocycles, peptides having 20– and 22–membered ring sizes (**3b**, IC_{50} = 15 nM and **3c**, IC_{50} = 14 nM, respectively) bound with greater affinities than those having 18– and 24–member ring sizes (**3a**, IC_{50} = 140 nM and **3d**, IC_{50} = 110 nM, respectively). For the type **4** macrocycles, affinities increased sequentially in going from the 15–membered to the 20–membered ring sizes (from **4a**, IC_{50} = 1.8 μM to **4c**, IC_{50} = 140 nM) and then decreased progressively as the ring size increased to 24–member (**4e**, IC_{50} = 13 μM). None of the type **5** macrocycles bound with good affinity (Table 1).

X-Ray Co-crystal Studies

To understand the effects of macrocyclization on PBD binding modes, we obtained the Plk1 PBD co-crystal structures of the highest affinity macrocycles (**3b**, **3c**, and **4c**) and compared these with the previously reported structure of the PBD-bound open-chain parent peptide **2** [Protein Data Bank (PDB) accession code 3RQ7].[4] By superimposing all structures using standard protocols included in MolSoft ICM Pro modeling software,[32,33] we found that folding of the flexible ring-closing polymethylene chains resulted in striking correspondence with **2** in the binding orientations of the peptide portions of all macrocycles (Figure 6). Interactions were preserved within the pThr-binding pocket with the key phosphoryl-binding

residues His538 and Lys540.[3,34] Consistent with previous reports that a hydrophobic region formed by the Trp414 and Phe535 residues are important in ligand binding,[3,34,35] we observed that for the current complexes, the largest contact interactions occurred with the Trp414 residue. The contact surface areas for **3b** and **3c** were larger than with the parent peptide **2**. Increased contact between the ligand Pro carbonyl and the Arg516 was also observed for **3b**. Contact with the Phe535 residue was increased for **3c**, where interactions with the ligand Pro pyrrolidine C4 and C5 methylenes as well as proximal components of the ring-closing chain were possible. In contrast, a dramatic loss of contact with Phe535 was incurred for **4c** due to the absence of a ligand Pro residue.

MATERIALS AND METHODS

Materials

Fmoc-Leu-OH, Fmoc-Ser(Trt)-OH and Fmoc-Thr(PO(OBzl)OH)-OH, NovaSyn®TGR amide resin and NovaSyn® TG Siber resin were purchased from Novabiochem. Allyl alcohol, 3-butenoic acid, 3-buten-1-ol, cinnamyl alcohol, 9-decenoic acid, 9-decen-1-ol, 5-hexenoic acid, 5-hexen-1-ol, 7-octenoic acid and 4-penten-1-ol were purchased from Sigma-Aldrich. 6-Hepten-1-ol, 7-octen-1-ol and 8-nonen-1-ol were purchased from Tokyo Chemical Industry Co., Ltd. (TCI). Fmoc-His(N(π)-$(CH_2)_8$Ph)-OH,[11] *N*-Fmoc (2*S*,4*R*)-4-(allyloxy)pyrrolidine-2-carboxylic acid,[36] *N*-Fmoc (2*S*,4*R*)-4-(pent-4-en-1-yloxy)pyrrolidine-2-carboxylic acid[36] and NBSH[26] were prepared according to the indicated literature procedures.

Solid-phase Peptide Synthesis

Resin-bound open chain peptides **6a** and **6b** (Figure 2) were synthesized on NovaSyn® TG Siber resin, while peptides **12a** and **12b** (Figure 3) and **16(a – c)** (Figure 4) were synthesized on NovaSyn®TGR resin following standard Fmoc-based solid-phase protocols using *N*-methyl-2-pyrrolidone (NMP) as solvent. 1-*O*-Benzotriazole-*N,N,N',N'*-tetramethyl-uronium-hexafluoro-phosphate (HBTU) (5.0 equiv), hydroxybenzotriazole (HOBT) (5.0 equiv) and *N,N*-diisopropylethylamine (DIPEA) (10.0 equiv) were used as coupling reagents. Amino terminal acetylation was achieved using 1-acetylimidazole (10 equiv) in DMF (4h) (for **6a** and **6b**), and appropriate alkenoic acids (5 equiv), HBTU (5.0 equiv), HOBt (5.0 equiv) and DIPEA (10 equiv) in NMP (2 h) [for **12a**, **12b** and **16 (a-c)**].

Detailed Solid-phase Protocol (Synthesis of Peptide 6a)—NovaSyn® TG Siber resin (0.21 mmol/g, 476 mg, 0.1 mmol) was swelled (CH_2Cl_2, 5 mL, 1 h) and then washed thoroughly with DMF (5 mL × 5). The N-Fmoc group was removed by treating with 20% piepridine in DMF (4 mL, 20 minutes) and the resin was then washed with DMF (5 mL × 6). A solution of Fmoc-Thr(PO(OBzl)OH)-OH (256 mg, 0.5 mmol), HBTU (195 mg, 0.5 mmol), HOBt (68 mg, 0.5 mmol) and DIPEA (0.174 mL, 1.0 mmol) in NMP (5 mL) was added and the resin was mixed by gentle rotation (2 h). The sequence of Fmoc-deprotection and coupling was completed with appropriate protected amino acids as specified in Materials. Following deprotection of the final residue, acetylation of the terminal amine was achieved using 1-acetylimidazole (110 mg, 1.0 mmol) in DMF (5 mL) (4 h). The resin was then washed with DMF (5 mL × 5); MeOH (5 mL × 5); CH_2Cl_2 (5 mL × 5) and diethyl ether

and the resin was dried under high vacuum to afford resin-bound peptide **6a** (0.1 mmol). The syntheses of resin-bound peptides **6b**, **12a**, **12b**, **16a**, **16b** and **16c** were achieved similarly using appropriate amino acids as indicated in Materials.

Resin Cleavage

NovaSyn® TGR Resin: Resin-bound peptide was cleaved by treatment with trifluoroacetic acid (TFA): triispropylsilane (TIS) : H_2O (95 : 2.5 : 2.5) at room temperature (4 h). The resin was removed by filtration and the filtrate was concentrated under vacuum. *NovaSyn® TG Siber Resin*: Resin bound peptide was cleaved by treatment with 1% TFA in CH_2Cl_2 at room temperature (5 min) and the resin was filtered and the filtrate collected. This procedure was repeated (5 x) and the combined filtrates were concentrated under vacuum.

HPLC Purification

Crude peptides (from 0.1 mmol resin) were dissolved in 50% aqueous CH_3CN (5 mL) and purified by reverse phase preparative HPLC using a Phenomenex C_{18} column (21 mm dia × 250 mm, cat. no: 00G-4436-P0) with a linear gradient from 30% aqueous CH_3CN (0.1% TFA) to 100% CH_3CN (0.1% TFA) over 30 min at a flow rate of 10.0 mL/min. Lyophilization gave the desired products as white amorphous solids.

On-resin Mistunobu N(τ)-His Alkylation

Resin-bound peptides **6a** and **6b** (Figure 2); **12a** and **12b** (Figure 3) and **16(a – c)** (Figure 4) (0.1 mmol) were treated with triphenylphosphine (PPh_3) (262 mg, 1.0 mmol), diethyl azidodicarboxylate (DEAD) (0.46 mL, 40% solution in toluene, 1.0 mol) and appropriate alcohols (1.0 mmol) in dry CH_2Cl_2 (4 mL) at room temperature (4 h). The resulting resin-bound peptides [**7(a – d)** (Figure 2); **13(b – e)** (Figure 3) or **17(a – f)** (Figure 4)] were washed sequentially with DMF, MeOH, CH_2Cl_2 and Et_2O and dried under vacuum.

On-resin Ring-closing Metathesis

To resin-bound peptide [**7(b – d)** (Figure 2); **13(b – e)** (Figure 3) or **17(a – f)** (Figure 4)] (0.1 mmol) under helium was added degassed CH_2Cl_2:DMF (1:1; 4 mL) and the resin was allowed to swell (30 min). A solution of Hoveyda-Grubbs 2nd generation catalyst (Aldrich cat. No. 569755) (18.8 mg, 0.03 mmol) in degassed CH_2Cl_2:DMF (10:1; 0.2 mL) was added and the mixture was stirred under microwave irradiation (120 °C; 30 min). The resulting resins [**8(b – d)**, Figure 2; **14(b – e)**, Figure 3 or **18(a – f)**, Figure 4] were washed sequentially with DMF, MeOH, CH_2Cl_2 and Et_2O and dried under vacuum.

Solution Phase Ring-closing Metathesis

Resin-bound open-chain peptide **7a** was cleaved from the resin and purified by HPLC as indicated above to yield peptide **10** (Figure 2). To the peptide under helium was added a solution of Hoveyda-Grubbs 2nd generation catalyst (0.5 equiv) 1 mM in degassed CH_2Cl_2:DMF (10:1) and the mixture was stirred at room temperature (24 h). Addition of catalyst (0.5 equiv) was repeated and the mixture was stirred at room temperature (24 h) and then concentrated under vacuum and purified by HPLC to yield **11a**.

On-resin Diimine Double Bond Reduction

To a solution of NBSH[26] (0.44 g, 1 mmol) in anhydrous CH_2Cl_2 (10 mL) was added Et_3N (0.56 mL, 2 mmol) and this was immediately added to resins [**8(b – d)**, Figure 2; **14(b – e)**, Figure 3 or **18(a – f)**, Figure 4] (0.05 mmol) under helium. The mixture was subjected to microwave irradiation (50 °C; 30 min). The resulting resins [**9(b – d)**, **15(b – e)** and **19(a – f)**, respectively] were washed sequentially with DMF, MeOH, CH_2Cl_2 and Et_2O and dried under vacuum. Resin cleavage and HPLC purification as indicated above provided the title peptides [**3c** and **3d; 4(b – e)** and **5(a – f)**, respectively].

Solution-Phase Double Bond Reduction (Hydrogenation)

A solution of alkene-containing peptide (**11a** and **11b**), 1 mM in DMF:THF (10:1) was hydrogenated over 10% Pd•C under H_2 at room temperature (overnight). The mixture was filtered and the filtrate was concentrated under vacuum and purified by HPLC to yield the title peptides **3a** and **3b**, respectively.

Mass Spectral Characterization

Low resolution, positive ion, electrospray ionization (ESI) mass spectra were obtained by LC/MS analysis on an Agilent LC/MSD single quadrupole system that was also equipped with an in-line diode-array ultraviolet (UV) detector. A narrow-bore (100 × 2.1 mm), small-particle (3.5-μm), Zorbax Rapid-Resolution reversed-phase C_{18} column coupled with a C_{18} guard column (12.5 × 2.1 mm) was eluted with a 5–90% gradient of MeOH:H_2O containing 0.1% AcOH at a flow rate of 300 μL/min to separate the components of crude reaction isolates and purified final products. Background-subtracted mass spectra and the appropriate compound-indicating extracted ion chromatograms were generated using the LC/MSD ChemStation software (version B.04.02 SP1).

High-resolution LC/MS and LC/MS/MS analyses were conducted on a Thermo-Fisher LTQ-XL Orbitrap hybrid mass spectrometer system operated under Xcalibur (version 2.1.0 SP1) control for data acquisition and qualitative analysis. A similar narrow-bore, small particle (3.5 μm) Zorbax Rapid-Resolution reversed-phase C_{18} column (100 × 2.1 mm) - guard column (12.5 × 2.1 mm) combination was eluted with CH_3CN:H_2O containing 0.1% AcOH at 250 μL/min. An initial linear gradient of 2–90% CH_3CN:H_2O over 15 min was followed by a 5 min isocratic hold at the final conditions before LC reset and equilibration (30 mi. cycle). Primary mass spectra (MS1) for accurate mass measurement of a molecular species ($[M+H]^+$, $[M+Na]^+$ or $[M+2H]^{+2}$) were obtained at a resolution of 30,0000 (full width at half maximum), while MS/MS (MS2) studies employing collision-induced dissociation (CID) or higher energy CID (HCD) were conducted at a resolution of 15,000. For these MS2 studies, $[M+H]^+$ or $[M+2H]^{+2}$ precursor ions were selected using a mass window that encompassed the isotopic profile of the ion of interest. For the compounds in question, CID and HCD were carried out at an optimized energy setting of 30 and 27.5, respectively, in order to give the highest intensity product ion mass spectrum. Product ion spectra containing multiply charged ions (i.e., those from $[M+2H]^{+2}$ precursors) were deconvoluted to a single charge state using the Xtract software module of Xcalibur in order to facilitate structural assignment and analysis. In the case of selected open-chain macrocyclic precursors (*e.g.*, compound **7c**), MS2 high-resolution extracted ion chromatograms (HR-XICs) were

generated post-analysis using a 20 or 30 mDa mass window centered on the observed accurate mass of the appropriate diagnostic ions. These HR-XICs were then used to locate and measure the relative amounts of isomeric bis-alkyl-His-containing phosphopeptide and esterified histidyl phosphopeptide present in the crude precyclized isolates. MS/MS structural assignments are as indicated in Figure 2, which is the MS/MS product ion mass spectrum resulting from the CID fragmentation of the $[M+H]^+$ ion of **3b**. A summary of the high resolution MS1 and MS2 data for each compound can be found in the Supporting Information.

X-ray Crystallography

Crystallization of Macrocycle-PBD Complexes—Plk1 PBD protein (residues 371–603) was obtained from Dr. Dan Lim who purified it as previously described.[3] Frozen stocks of protein at 37 mg/mL in 10 mM Tris pH 8, 0.5 M NaCl, 10 mM dithiothreitol (DTT)were thawed and diluted to 10 mg/mL with the same buffer. Complexes with each of three macrocycle compounds (**3b**, **3c** and **4b**) were prepared by adding 100 mM stocks of the macrocycle in dimethylsulfoxide (DMSO) directly to the diluted protein to achieve a final concentration of 1 mM. Crystals were grown by hanging drop vapor diffusion, with drops made by mixing equal volumes of protein-macrocycle complex and well solution containing 2–6% polyethylene glycol (PEG)-3350. Crystals were cryo-protected by quickly dipping in a solution of 37.5% ethylene glycol in well solution and frozen in liquid nitrogen.

Structure Solution and Refinement—X-ray diffraction data were collected at the Advance Proton Source (APS) using the Northeastern Collaborative Access Team (NE-CAT) 24-ID-C beam line. Data were indexed, integrated and scaled using HKL2000.[37] All crystals belonged to the space group $P2_1$ with nearly identical unit cell parameters. The structures were solved by molecular replacement using PHASER[38] with PDB entry 4DFW (minus solvent and bound ligand) as a search model. The models were built with COOT[39] and refined using PHENIX.[40] Refinement constraints for the bound macrocycle ligands were generated by the GRADE web server (http://grade.globalphasing.org). Data collection and refinement statistics are in the Supporting Information.

ELISA-based PBD-binding Inhibition Assays

Similar to previously reported procedures,[3,4] biotinylated p-T78 peptide was first diluted with 1 × coating solution (KPL Inc., Gaithersburg, MD) to the final concentration of 0.3 μM, and then 100 μL of the resulting solution was immobilized onto a 96-well streptavidin-coated plate (Nalgene Nunc, Rochester, NY). The wells were washed once with phosphate buffered saline (PBS) plus 0.05% Tween20 (PBST), and incubated with 200 μL of PBS plus 1% bovine serum albumin (BSA) (blocking buffer) for 1 h to prevent non-specific binding. Mitotic 293A lysates expressing HA-EGFP-Plk1 were prepared in TBSN buffer [20mM Tris-Cl (pH 8.0), 150 mM NaCl, 0.5% Nonidet P-40, 5 mM EGTA, 1.5 mM EDTA, 20 mM *p*-nitrophenyl phosphate, and protease inhibitor mixture (Roche)] (~ 60 μg total lysates in 100 μl buffer), mixed with the indicated amount of the competitors (p-T78 peptide and its derivative compounds), provided immediately onto the biotinylated peptide-coated ELISA wells, and then incubated with constant rocking for 1 h at 25 °C. Following the incubation, ELISA plates were washed 4 × with PBST. To detect bound HA-EGFP-Plk1, the plates were

probed for 2 h with 100 μL/well of anti-HA antibody at a concentration of 0.5 μg/mL in blocking buffer and then washed 5 ×. The plates were further probed for 1 h with100 μL/well of horse radish peroxidase (HRP)-conjugated secondary antibody (GE Healthcare, Piscataway, NJ) at a 1:1,000 dilution in blocking buffer. The plates were washed 5 × with PBST and incubated with 100 μL/well of 3,3′,5,5′-tetramethylbenzidine (TMB) solution (Sigma, St. Louis, MO) as a substrate until a desired absorbance was reached. The reactions were stopped by the addition of 100 μL/well of stop solution (Cell Signaling Technology, Danvers, MA). The optical density (O.D.) was measured at 450 nm by using an ELISA plate reader (Molecular Devices, Sunnyvale, CA). Calculated IC_{50} values are listed in Figure 1 and Table 1.

CONCLUSION

The ability of neighboring acidic residues to facilitate Mitsunobu N(τ)–alkylation of His residues bearing an N(π)–alkyl group provides a useful means of specific structural modification that opens a range of applications. Our use of the bis-alkyl-His imidazolium ring for the synthesis of charge-masked macrocyclic phosphopeptides provides one example of an application to biologically important protein-protein interactions.

Supplementary Material

Refer to Web version on PubMed Central for supplementary material.

Acknowledgments

This work was supported in part by the Intramural Research Program of the NIH, Center for Cancer Research, NCI-Frederick and the National Cancer Institute, National Institutes of Health (W.-J. Q., J.-E. P., C. C. L., J. A. K., K. S. L. and T. R. B.), an NCI Director's Innovation Career Development Award (W.-J. Q.) and National Institutes of Health grants ES015339 and GM104047 (M. B. Y.). This work is based upon research conducted at the Advanced Photon Source on the Northeastern Collaborative Access Team beamlines, which are supported by a grant from the National Institute of General Medical Sciences (P41 GM103403) from the National Institutes of Health. Use of the Advanced Photon Source, an Office of Science User Facility operated for the U.S. Department of Energy (DOE) Office of Science by Argonne National Laboratory, was supported by the U.S. DOE under Contract No. DE-AC02-06CH11357. Appreciation is expressed to Wei Dai, New York University School of Medicine, NY for reagents and to Dan Lim of the David H. Koch Institute for Integrative Cancer Research for providing purified Plk-1 PBD.

References

1. Qian W-J, Park J-E, Lim D, Lai CC, Kelley JA, Park S-Y, Lee KW, Yaffe MB, Lee KS, Burke TR. Biopolymers Pept Sci. 2014; 102:444–455.
2. Qian W-J, Burke TR Jr. Org Biomol Chem. 2015; 13:4221–4225. [PubMed: 25739367]
3. Yun S-M, Moulaei T, Lim D, Bang JK, Park J-E, Shenoy SR, Liu F, Kang YH, Liao C, Soung N-K, Lee S, Yoon D-Y, Lim Y, Lee D-H, Otaka A, Appella E, McMahon JB, Nicklaus MC, Burke TR Jr, Yaffe MB, Wlodawer A, Lee KS. Nat Struct Mol Biol. 2009; 16:876–882. [PubMed: 19597481]
4. Liu F, Park J-E, Qian W-J, Lim D, Graber M, Berg T, Yaffe MB, Lee KS, Burke TR Jr. Nat Chem Biol. 2011; 7:595–601. [PubMed: 21765407]
5. Allentoff AJ, Mandiyan S, Liang H, Yuryev A, Vlattas I, Duelfer T, Sytwu I-I, Wennogle LP. Cell Biochem Biophys. 1999; 31:129–140. [PubMed: 10593255]
6. Davies JS. J Pept Sci. 2003; 9:471–501. [PubMed: 12952390]
7. Jiang S, Li Z, Ding K, Roller PP. Curr Org Chem. 2008; 12:1502–1542.
8. White CJ, Yudin AK. Nat Chem. 2011; 3:509–524. [PubMed: 21697871]

9. Dharanipragada R. Future Med Chem. 2013; 5:831–849. [PubMed: 23651095]
10. Murugan RN, Park J-E, Lim D, Ahn M, Cheong C, Kwon T, Nam K-Y, Choi SH, Kim BY, Yoon D-Y, Yaffe MB, Yu D-Y, Lee KS, Bang JK. Bioorg Med Chem. 2013; 21:2623–2634. [PubMed: 23498919]
11. Qian W, Liu F, Burke TR Jr. J Org Chem. 2011; 76:8885–8890. [PubMed: 21950469]
12. Blackwell HE, Sadowsky JD, Howard RJ, Sampson JN, Chao JA, Steinmetz WE, O'Leary DJ, Grubbs RH. J Org Chem. 2001; 66:5291–5302. [PubMed: 11485448]
13. Liu F, Giubellino A, Simister PC, Qian W, Giano MC, Feller SM, Bottaro DP, Burke TR Jr. Biopolymers. 2011; 96:780–788. [PubMed: 21830199]
14. Chapman RN, Arora PS. Org Lett. 2006; 8:5825–5828. [PubMed: 17134282]
15. Robinson AJ, Elaridi J, Van Lierop BJ, Mujcinovic S, Jackson WR. J Pept Sci. 2007; 13:280–285. [PubMed: 17394122]
16. Robinson AJ, van Lierop BJ, Garland RD, Teoh E, Elaridi J, Illesinghe JP, Jackson WR. Chem Commun. 2009:4293–4295.
17. García-Aranda MI, Marrero P, Gautier B, Martín-Martínez M, Inguimbert N, Vidal M, García-López MT, Jiménez MA, González-Muñiz R, Vega MJPD. Bioorg Med Chem. 2011; 19:1978–1986. [PubMed: 21349728]
18. Mulder MPC, Kruijtzer JAW, Breukink EJ, Kemmink J, Pieters RJ, Liskamp RM. J Bioorg Med Chem. 2011; 19:6505–6517.
19. Heapy AM, Williams GM, Fraser JD, Brimble MA. Org Lett. 2012; 14:878–881. [PubMed: 22239540]
20. Scholl M, Ding S, Lee CW, Grubbs RH. Org Lett. 1999; 1:953–956. [PubMed: 10823227]
21. Garber SB, Kingsbury JS, Gray BL, Hoveyda AH. J Am Chem Soc. 2000; 122:8168–8179.
22. Michalak M, Wicha J. Org Biomol Chem. 2011; 9:3439–3446. [PubMed: 21424020]
23. Stoianova DS, Hanson PR. Org Lett. 2000; 2:1769–1772. [PubMed: 10880222]
24. Heckrodt TJ, Singh R. Synth Commun. 2012; 42:2854–2865.
25. Maysuya Y, Takayanagi S-I, Nemoto H. Chem - Eur J. 2008; 14:5275–5281. [PubMed: 18442032]
26. Buszek KR, Brown NJ. Org Chem. 2007; 72:3125–3128.
27. García-Aranda MI, González-Muñiz R, García-López MT, Pérez de Vega MJ. Eur J Org Chem. 2009; 2009:4149–4157.
28. Palumbo AM, Tepe JJ, Reid GE. J Proteome Res. 2008; 7:771–779. [PubMed: 18181561]
29. Boersema PJ, Mohammed S, Heck AJR. J Mass Spectrom. 2009; 44:861–878. [PubMed: 19504542]
30. Bythell BJ, Suhai S, Somogyi Á, Paizs B. J Am Chem Soc. 2009; 131:14057–14065. [PubMed: 19746933]
31. Kang YH, Park J-E, Yu L-R, Soung N-K, Yun S-M, Bang JK, Seong Y-S, Yu H, Garfield S, Veenstra TD, Lee KS. Mol Cell. 2006; 24:409–422. [PubMed: 17081991]
32. ICM Pro Software v3.8-0/MacOSX. MolSoft LLC; La Jolla, CA: http://www.molsoft.com
33. Abagyan, R.; Orry, A.; Raush, E.; Totrov, M. ICM-Chemist-Pro User Guide v38. http://wwwmolsoftcom/chemistpro/
34. Elia AE, Rellos P, Haire LF, Chao JW, Ivins FJ, Hoepker K, Mohammad D, Cantley LC, Smerdon SJ, Yaffe MB. Cell. 2003; 115:83–95. [PubMed: 14532005]
35. Murugan RN, Ahn M, Lee WC, Kim H-Y, Song JH, Cheong C, Hwang E, Seo J-H, Shin SY, Choi SH, Park J-E, Bang JK. PLoS One. 2013; 8:e80043. [PubMed: 24223211]
36. Peters C, Bacher M, Buenemann CL, Kricek F, Rondeau J-M, Weigand K. Chem Bio Chem. 2007; 8:1785–1789.
37. Otwinowski, Z.; Minor, W. Macromolecular Crystallography, Part A. Carter, CW., Jr; Sweet, RM., editors. Academic Press; New York, NY: 1997. p. 307-326.
38. McCoy AJ, Grosse-Kunstleve RW, Adams PD, Winn MD, Storoni LC, Read RJ. J Appl Cryst. 2007; 40:658–674. [PubMed: 19461840]
39. Emsley P, Cowtan K. Acta Crystallogr D Biol Crystallogr. 2004; 60:2126–2132. [PubMed: 15572765]

40. Adams PD, Afonine PV, Bunkoczi G, Chen VB, Davis IW, Echols N, Headd JJ, Hung LW, Kapral GJ, Grosse-Kunstleve RW, McCoy AJ, Moriarty NW, Oeffner R, Read RJ, Richardson DC, Richardson JS, Terwilliger TC, Zwart PH. Acta Crystallogr D Biol Crystallogr. 2010; 66:213–221. [PubMed: 20124702]

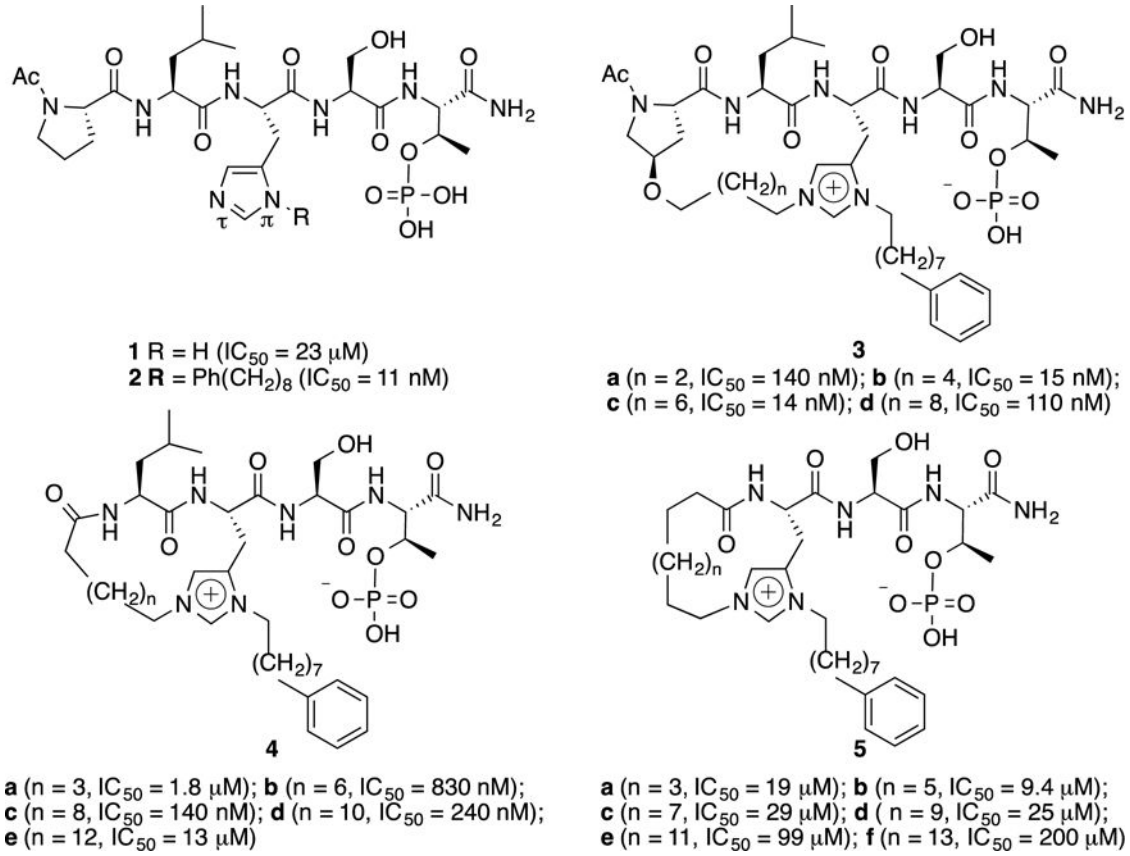

Figure 1.
Structures of target PBD-binding peptides with Plk1 PBD-binding affinities.

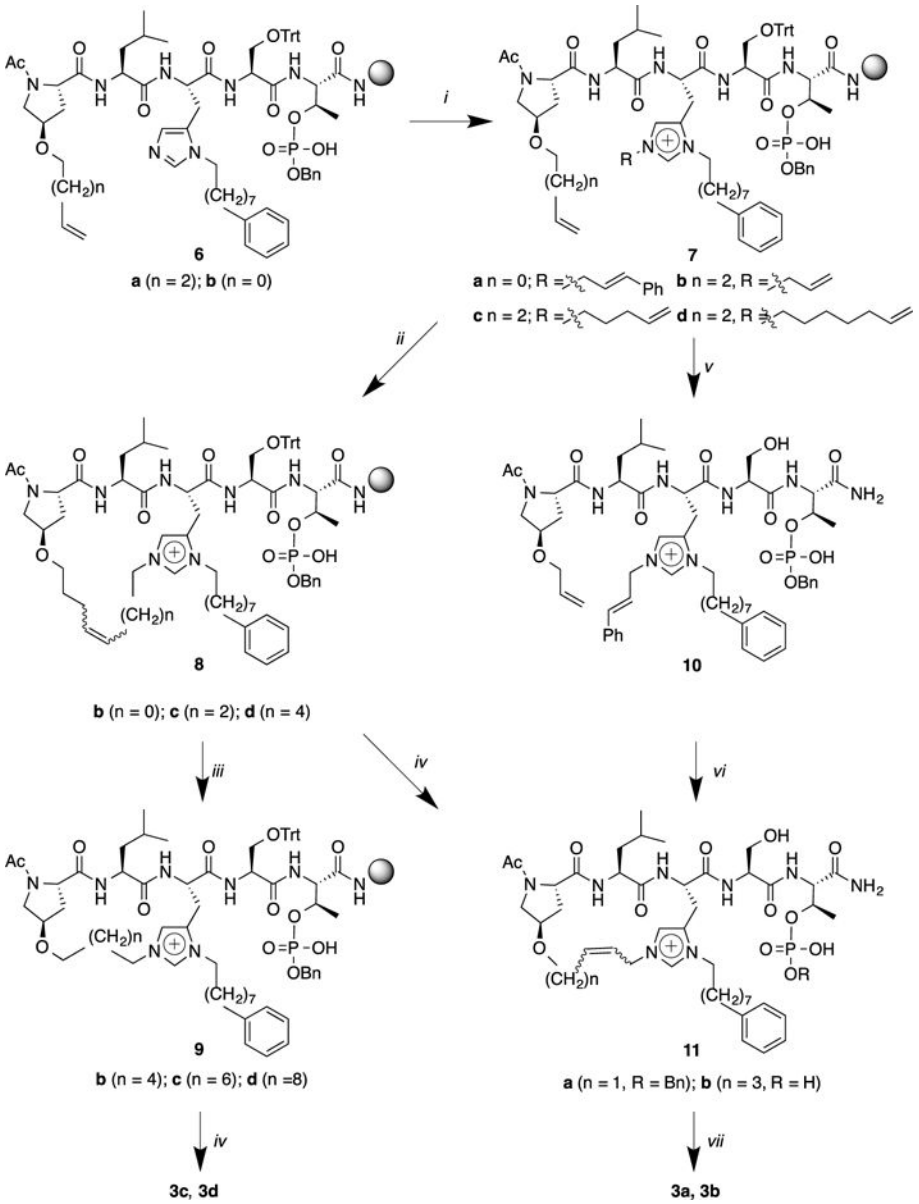

Figure 2. Reagents and Conditions

i) ROH (10 eq.), PPh_3 (10.0 eq.), DEAD (10.0 eq.), CH_2Cl_2, 4 h; *ii*) Hoveyda-Grubbs 2nd generation cat. (0.3 eq.), CH_2Cl_2/DMF (10:1, degassed), microwave, 120 °C, 30 min; *iii*) NBSH (20 eq.), Et_3N (40 eq.), CH_2Cl_2, microwave, 50 °C, 30min; *iv*) TFA/H_2O/TIS = 95: 2.5: 2.5, 4 h; *v*) 1% TFA in CH_2Cl_2; *vi*)) Hoveyda-Grubbs 2nd generation cat. (0.5 eq.), CH_2Cl_2/DMF (10:1, degassed), room temp., 24 h (two-times); *vii*) H_2, 10% Pd•C, THF/DMF (10:1), overnight.

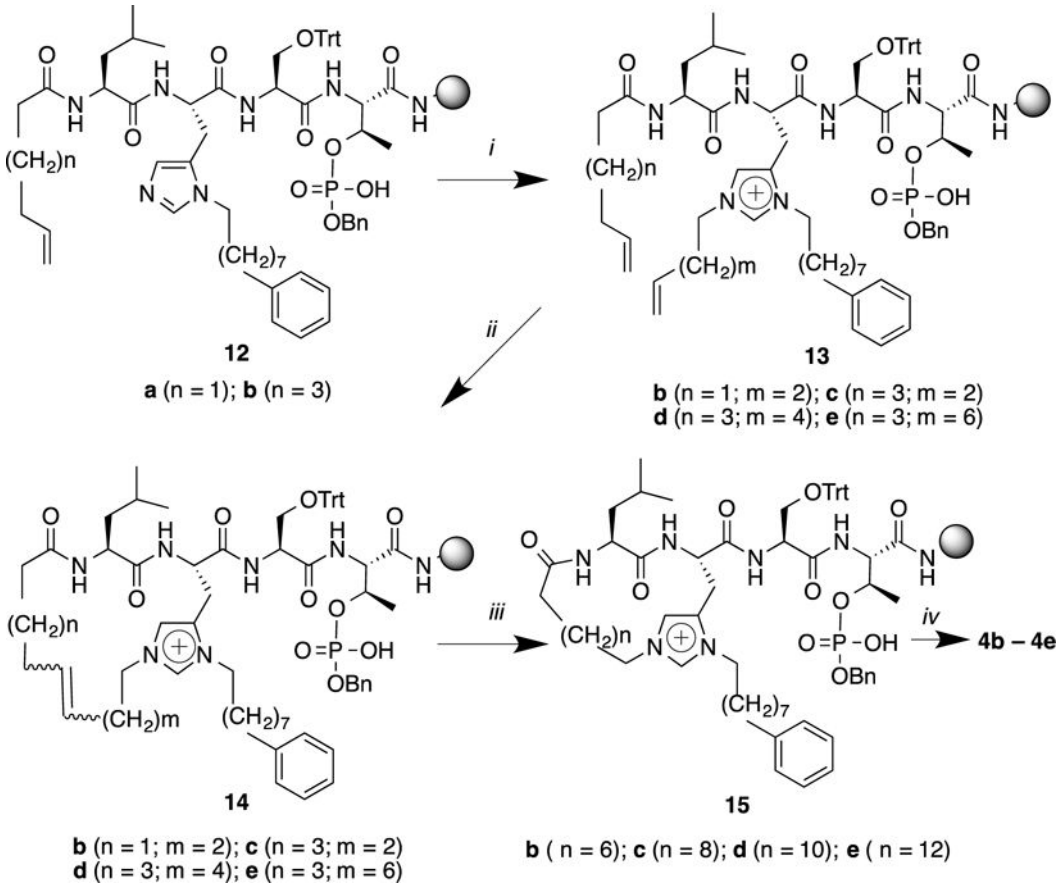

Figure 3. Reagents and Conditions

i) ROH (10 eq.), PPh_3 (10.0 eq.), DEAD (10.0 eq.), CH_2Cl_2, 4 h; *ii*) Hoveyda-Grubbs 2nd generation cat. (0.3 eq.), CH_2Cl_2/DMF (10:1, degassed), microwave, 120 °C, 30 min; *iii*) NBSH (20 eq.), Et_3N (40 eq.), CH_2Cl_2, microwave, 50 °C, 30 min; *iv*) TFA/H_2O/TIS = 95: 2.5: 2.5, 4 h.

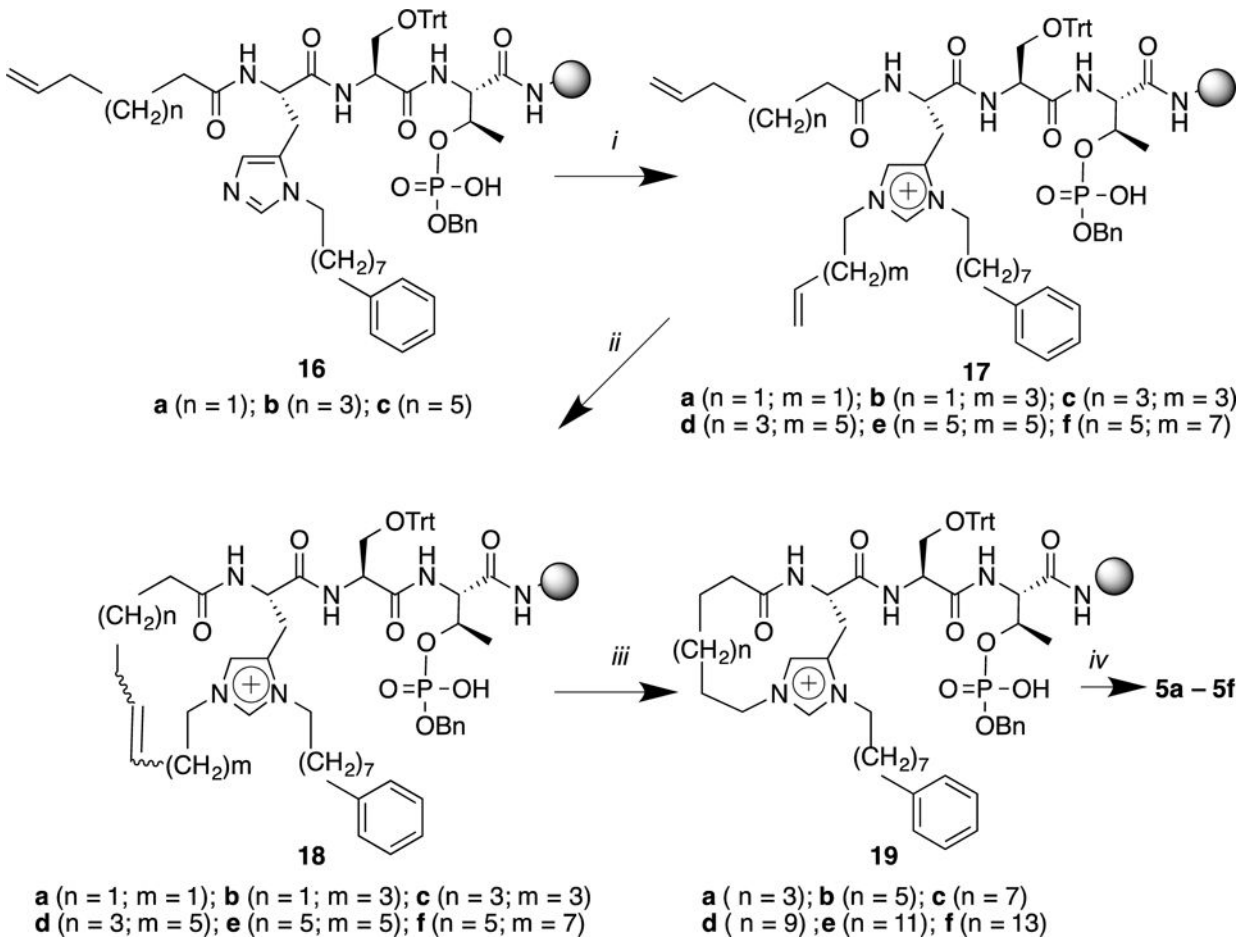

Figure 4. Reagents and Conditions

i) ROH (10 eq.), PPh_3 (10.0 eq.), DEAD (10.0 eq.), CH_2Cl_2, 4 h; *ii*) Hoveyda-Grubbs 2nd generation cat. (0.3 eq.), CH_2Cl_2/DMF (10:1, degassed), microwave, 120 °C, 30 min; *iii*) NBSH (20 eq.), Et_3N (40 eq.), CH_2Cl_2, microwave, 50 °C, 30 min; *iv*) TFA/H_2O/TIS = 95: 2.5: 2.5, 4 h.

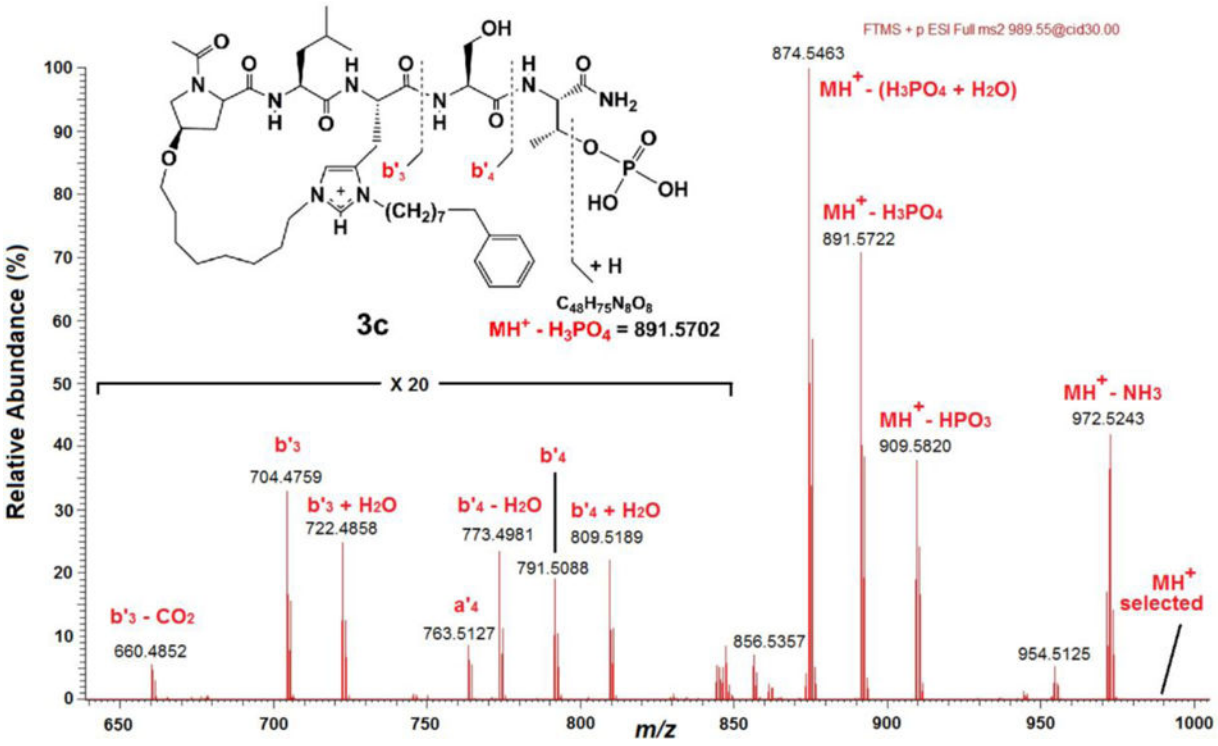

Figure 5.

Partial, high resolution, CID MS/MS mass spectrum of the MH^+ of **3c**. The presence of a free phosphate moiety is indicated by the product ions corresponding to MH^+-HPO_3, MH^+-H_3PO_4, and MH^+-(H_3PO_4 + NH_3). Insert: Structure and expected CID fragmentation of the MH^+ (*m/z* 989.5471) of **3c**.

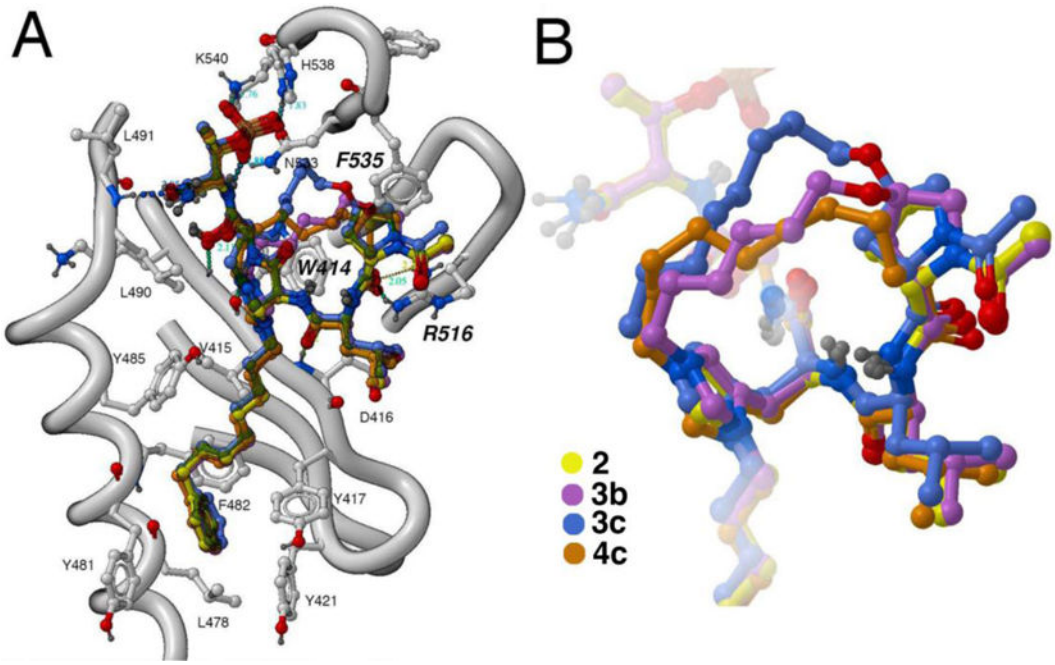

Figure 6.

X-ray crystal structures of Plk1 PBD-bound ligands. (A) Protein ribbon rendition of PBD-bound **2** (PDB: 3RQ7) with key interacting protein residues shown and the structures of PBD-bound macrocycles **3b**, **3c** and **4c** superimposed. (B) Enlargement of overlaid PBD-bound peptides shown in (A). For both (A) and (B) ligand coloring is as indicated.

Table 1

Plk1 PBD IC_{50} values measured in an ELISA competition assay.[a]

No.	Ring Size	IC_{50} (μM)
1	–	29
2	–	0.011
3a	18	0.14
3b	20	0.015
3c	22	0.014
3d	24	0.11
4a	15	1.8
4b	18	0.83
4c	20	0.14
4d	22	0.24
4e	24	13
5a	14	19
5b	16	9.4
5c	18	29
5d	20	25
5e	22	99
5f	24	200

[a]Values were obtained in an ELISA-based assay that measured the ability of peptides to compete with an immobilized pT78 peptide for binding to HEK 293A cell lysate-derived GFP-HA-fused Plk1.